ACS OMEGA

http://pubs.acs.org/journal/acsodf

Article

Comparative Studies on the Structure–Performance Relationships of Phenothiazine-Based Organic Dyes for Dye-Sensitized Solar Cells

Shengzhong Li, Jingwen He, Huiyun Jiang, Shu Mei, Zhenguang Hu, Xiangfei Kong, Miao Yang, Yongzhen Wu,* Shuhua Zhang,* and Haijun Tan*

Cite This: *ACS Omega* 2021, 6, 6817–6823

Read Online

ACCESS | Metrics & More | Article Recommendations | Supporting Information

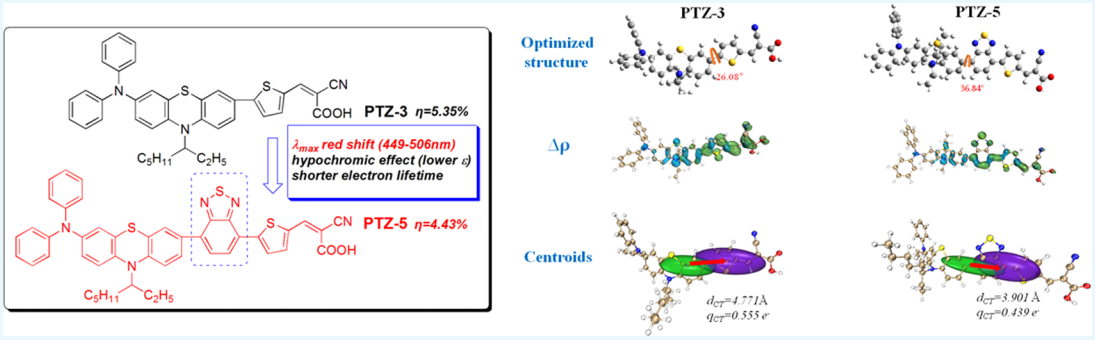

ABSTRACT: A D–A–π–A dye (**PTZ-5**) has been synthesized by introducing a benzothiadiazole (BTD) unit as an auxiliary acceptor in a phenothiazine-based D–π–A dye(**PTZ-3**) to broaden its spectral response range and improve the device performance. Photophysical properties indicate that the inclusion of BTD in the **PTZ-5** effectively red-shifted the absorption spectra by reducing the E_{gap}. However, the device measurements show that the open-circuit voltage (V_{oc}) of **PTZ-5** cell (640 mV) is obviously lower than that of the **PTZ-3** cell (710 mV). This results in a poor photoelectric conversion efficiency (PCE) (4.43%) compared to that of **PTZ-3** cell (5.53%). Through further comparative analysis, we found that the introduction of BTD increases the dihedral angle between the D and A unit, which can reduce the efficiency of intramolecular charge transfer (ICT), lead to a less q_{CT} and lower molar extinction coefficient of **PTZ-5**. In addition, the ESI test found that the lifetime of the electrons in the **PTZ-5** cell is shorter. These are the main factors for the above unexpected result of PCE. Our studies bring new insights into the development of phenothiazine-based highly efficient dye-sensitized solar cells (DSSCs).

INTRODUCTION

Dye-sensitized solar cells (DSSCs) have received massive attention due to their simple structure and low cost.[1] Novel and highly efficient dyes play a decisive role in developing efficient DSSCs. Since the pioneering work of Grätzel,[1] numerous researchers have done a lot of research work in dye development.[2−5] At present, thousands of dyes have been applied to DSSCs, mainly concentrated in porphyrin,[6−8] ruthenium complexes,[9,10] and metal-free pure organic dyes.[11−20] As early as in 2015, Kakiage et al. reported a fantastic photoelectric conversion efficiency (PCE) of 14.34% using co-sensitization of silyl-anchor-based organic dye (ADEKA-1) and carboxy-anchor-based organic dye (LEG-4).[21] In 2019, Sun et al. designed and synthesized organic dye ZL003, which achieved a relatively high PCE of 13.6% due to minimal energy losses on molecular excitation.[22] Recently, Kim et al. have also shown a striking PCE of 14.2% by co-sensitizing novel thieno-[3,2-b]indole-based organic dye and a porphyrin sensitizer.[23]

Compared with metal complex dyes, metal-free pure organic dyes have the advantages of high molar extinction coefficient, easy structure modification, and adjustable spectral response range.[24−26] The incipient design of organic dyes for DSSC is based on the donor–π–conjugated-bridge-acceptor (D–π–A) structure.[27,28] The push–pull structure is formed between the electron donor and the acceptor, which facilitates the injection of electrons. However, the limitations of spectral response are still the deficiency of D–π–A dye molecules. In 2011, Zhu et al. innovatively proposed the concept of donor-acceptor–π–bridge-acceptor (D–A–π–A).[15,29−33] They introduced an auxiliary acceptor such as benzotriazole, quinoxaline, benzothiadiazole (BTD), and benzoxadiazole to the traditional

Received: December 2, 2020
Accepted: February 22, 2021
Published: March 4, 2021

https://dx.doi.org/10.1021/acsomega.0c05887
ACS Omega 2021, 6, 6817–6823

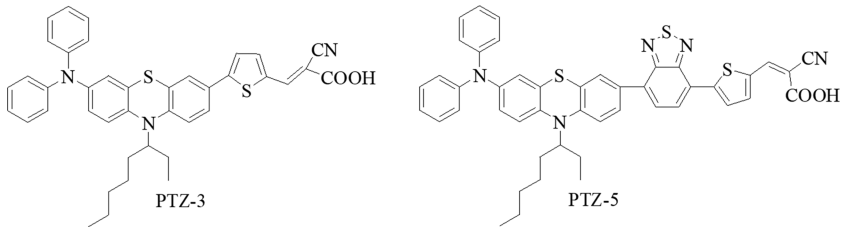

Figure 1. Molecular structures of the **PTZ-3** and **PTZ-5**.

D−π−A-type molecules, which can reduce the molecular optical band gap and broaden the spectral response range.[34−37]

Inspired by the above works. Here, we have synthesized two phenothiazine-based organic dyes, **PTZ-3** (D−π−A) and **PTZ-5** (D−A−π−A). As shown in Figure 1, compared to **PTZ-3**, a benzothiadiazole was added as an auxiliary acceptor to **PTZ-5** to broaden the spectral response range and improve the device performance. We also investigated the structure−performance relationships of these two dyes. The relationships between the structure and the performance gleaned from our study bring new insight into the further research of phenothiazine-based organic dyes in DSSCs.

RESULTS AND DISCUSSION

Synthesis. The synthetic route of **PTZ-3** and **PTZ-5** are shown in Scheme S1. These two dyes were synthesized by C−N coupling, brominating, Suzuki cross-coupling, and Knoevenagel reactions. All of the solvents, original materials, and reagents were purchased commercially and used as received without further purification. The specific synthesis steps of compound **1** refer to our previous work.[38] The synthetic details and characteristic results for the intermediates and target dyes are provided in the Supporting Information (SI).

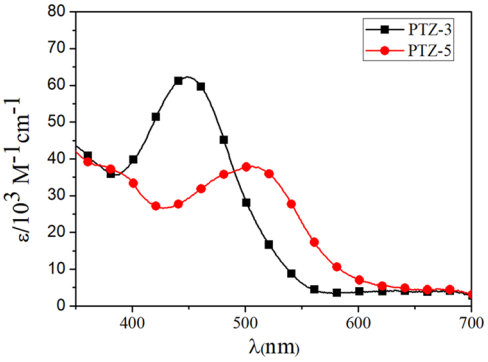

Figure 2. UV−vis absorption spectra of **PTZ-3** and **PTZ-5** in THF.

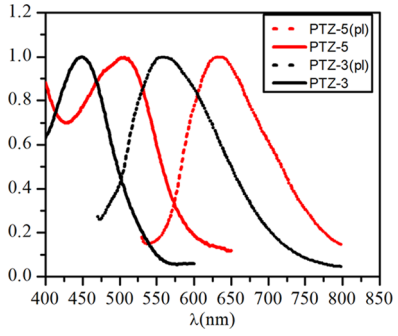

Figure 3. Normalized electronic absorption and emission spectra of **PTZ-3** and **PTZ-5** in THF.

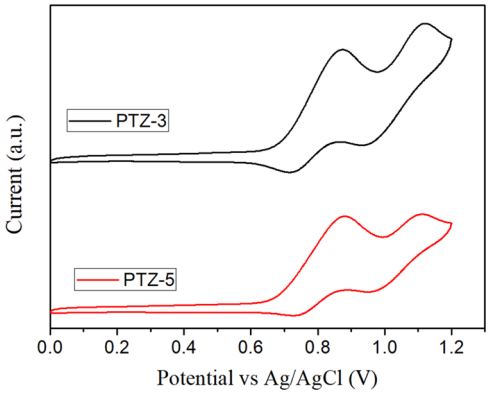

Figure 4. Cyclic voltammetry of **PTZ-3** and **PTZ-5** in THF.

Photophysical and Electrochemical Properties. Figure 2 shows the UV−vis absorption spectra of **PTZ-3** and **PTZ-5** dissolved in tetrahydrofuran (THF). We found that the spectral response of **PTZ-5** is significantly red-shifted to 57 nm, which is probably due to the auxiliary acceptor presence compared with that of **PTZ-3**. Furthermore, **PTZ-3** exhibits a higher molar extinction coefficient compared with **PTZ-5**, which were 62.3 × 10^3 and 38 × 10^3 $M^{-1}\cdot cm^{-1}$, respectively. The UV−vis absorption spectra and the steady-state fluorescence emission spectra were processed using a normalized method, as shown in Figure 3. The spectral intersections of the dye molecules **PTZ-3** and **PTZ-5** are at positions of 503 and 544 nm, respectively. According to the transition band gap formula: E_{0-0} = 1240/λ, the calculated band gap width (E_{0-0}) is 2.5 and 2.28 eV, respectively. The results demonstrate that the introduction of benzothiadiazole unit leads to a smaller band gap and a broader spectral response range.

The adaptation of energy level between the dye molecules, semiconductor conduction band (CB), and the redox electrolyte is the basis for the manufacture of DSSCs. The ground-state oxidation−reduction potential (E_{D/D^+}) of the two dyes can be derived from the cyclic voltammetry (CV) curve (Figure 4), which were measured in THF with the Fc/Fc^+ redox couple as a reference. The E_{D/D^+} for **PTZ-3** and **PTZ-5** are 0.23 and 0.21 V, respectively. The excited state redox potential (E_{D^*/D^+}) of the dye molecules **PTZ-3** and **PTZ-5** are obtained according to the formula ($E_{D^*/D^+} = E_{D/D^+} - E_{0-0}/e$) are −2.27 and −2.07 V, respectively (no entropy changes are considered during light excitation). Table 1 summarizes the relevant parameters.

Theoretical Calculation. The intrinsic electronic structures of the dyes such as the distribution of the highest occupied molecular orbitals (HOMOs) and the lowest

https://dx.doi.org/10.1021/acsomega.0c05887
ACS Omega 2021, 6, 6817−6823

Table 1. Photophysical and Electrochemical Data of PTZ-3 and PTZ-5

dye	λ_{max}^{abs} [a] (nm)	ε_{max}^{abs} [a] (10^3 M^{-1} cm^{-1})	λ_{max}^{pl} [a] (nm)	E_{0-0} [b] (eV)	E_{D/D^+} [c] (V)	E_{D^*/D^+} [d] (V)
PTZ-3	449	62.3	558	2.5	0.23	−2.27
PTZ-5	506	38	635	2.28	0.21	−2.07

[a]The maximum absorption wavelength (λ_{max}^{abs}), the maximum molar absorption coefficient (ε_{max}^{abs}), and the maximum emission wavelength (λ_{max}^{pl}) were derived from the steady-state absorption−emission spectra of the dye in THF. The molar absorption coefficient (ε) were calculated by the equation $\varepsilon = A/(cl)$, where A is the absorbance, c is the concentration in moles per liter, and l is the path length in centimeters. [b]The 0−0 transition energy (E_{0-0}) was estimated from the intersection of the normalized absorption and the emission spectra. [c]The ground-state redox electricity (E_{D/D^+}) was referenced to Fc/Fc^+. [d]The excited redox potential (E_{D^*/D^+}) was derived from the formula $E_{D^*/D^+} = E_{D/D^+} - E_{0-0}/e$ without considering the entropy change in the light excitation process.

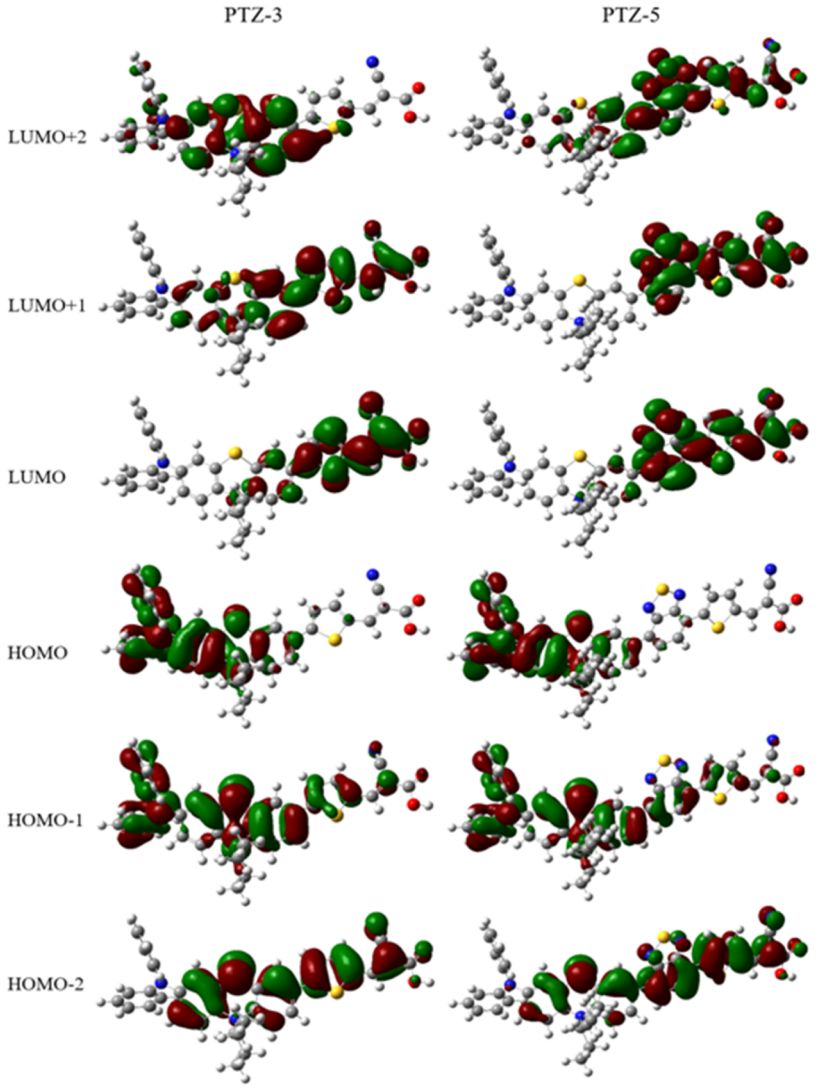

Figure 5. Electron cloud distribution of **PTZ-3** and **PTZ-5** at the B3LYP/6-31G(d,p) level with Gaussian 09.

unoccupied molecular orbitals (LUMOs) affect the intramolecular charge transfer (ICT) and excitation characteristics. As shown in Figure 5, the HOMOs of **PTZ-3** and **PTZ-5** are distributed on the donor units, while the LUMOs are primarily localized on the π−A or A−π−A units. The simulated UV−vis absorption spectra of the dyes in the THF solvent are presented in Figure 6. There are two distinct absorption bands in the UV and visible regions. The absorption from 200 to 400 nm can be described by π−π^* electronic transitions and the range 400−700 nm corresponds to the ICT process from the donor unit (HOMO) to the acceptor unit (LUMO) of dyes. The calculated maximum absorption wavelengths of **PTZ-3** and **PTZ-5** are 446 and 504 nm, respectively. This is quite consistent with the results of the spectral test. Table 2 shows the values for the specific parameters of these two dyes. Notably, the calculated oscillator strengths (f) of the $S_0 \rightarrow S_1$ for dye **PTZ-5** is lower than that of dye **PTZ-3**.

Then, we analyzed the intermolecular charge transfer (ICT) characteristics for further exploration. As shown in Figure 7 and Table 3, the introduction of BTD on the one hand can improve the H index (the half sum of the centroid axis length along the D−A direction) of **PTZ-5** to strengthen the hole and electron transfer and on the other hand can slightly reduce the molecular d_{CT} by reducing the E_{gap}, which is also reflected in

https://dx.doi.org/10.1021/acsomega.0c05887
ACS Omega 2021, 6, 6817−6823

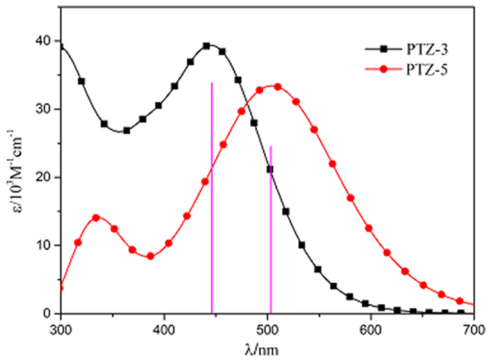

Figure 6. Absorption spectra of **PTZ-3** and **PTZ-5** at the time-dependent TD-B3LYP/6-31G(d) level with Gaussian 09.

the hole (blue)−electron (green) distribution map ($\Delta\rho$) and charge density difference map (centroids). It is a reasonable diagnostic index to quantify through the space transitions, which denotes a substantial charge separation if it has a positive value.[39] However, the t of **PTZ-5** is a negative number. Also, it can be seen from the optimized structure from Figure 7 that the introduction of BTD increases the dihedral angle between the D−A units and affects the effective transfer of excitation charges from D to A (HOMO to LUMO), thereby reducing the q_{CT} (amount of transfer electrons) of **PTZ-5**. This produced a hypochromic effect and resulted in a lower molar extinction coefficient of **PTZ-5**. This eventually affects the performance of the device.

Photovoltaic Performance. Figure 8 shows the incident photon-to-current conversion efficiency (IPCE) of the devices. The results reveal that the IPCE of the **PTZ-3** cell are higher than that of **PTZ-5** in the range of 300−560 nm. Also, the IPCE maximum value of **PTZ-5** cell is 58%, which is significantly lower than that of the **PTZ-3** cell (78%). This phenomenon is probably due to the higher molar extinction coefficient for **PTZ-3** than that for **PTZ-5** in this region. Nevertheless, the IPCE of the **PTZ-5** cell has a broadened IPCE spectrum response than the **PTZ-3** cell, with the maximum reaching 800 nm, which is probably due to the introduction of benzothiadiazole, and exhibits a broadened absorption spectrum for **PTZ-5**.

The photocurrent density−voltage (J−V) characteristics were recorded under simulated AM 1.5 G illumination, and the charts are given in Figure 9 and Table 4. The results reveal that the open-circuit voltage (V_{oc}, 710 mV) of the **PTZ-3** cell is significantly higher than that of **PTZ-5** (V_{oc}, 640 mV). In the end, the photoelectric conversion efficiency (PCE) of the **PTZ-3** cell is 5.35%, which is higher than that of **PTZ-5** (PCE = 4.43%). This result is consistent with the previous IPCE analysis.

Then, the electrochemical impedance spectroscopy (EIS) analysis was carried out in the dark with a series of bias voltages around their V_{oc} values to gain insights into the differences in V_{oc} of these two devices. In general, the V_{oc} was determined by the quasi-Fermi level ($E_{F,n}$) of TiO_2 and the potentials of the electrolyte. Since we have a fixed electrolyte in this work, the conduction band (CB) position and the injected electron density in TiO_2 will be the main factors that affect V_{oc}. It can be seen from Figure 10, at a fixed potential, the capacitance values of **PTZ-3**- and **PTZ-5**-based devices are almost the same, suggesting a negligible influence of the CB shift on V_{oc} variation. Ultimately, we found that the electron lifetime, which can reflect the injected electron density was the real main factor for determining V_{oc}. As shown in Figure 10, under the same bias voltage, the electron lifetime of **PTZ-3** cell was significantly longer than that of the **PTZ-5** cell, which is in line with the V_{oc} difference.

Therefore, we consider that the lower q_{CT} and molar extinction coefficient of dye and shorter electron lifetime in the device were the critical reasons for the poor performance of the **PTZ-5** cell.

CONCLUSIONS

In summary, we have done comparative research about the influence of benzothiadiazole unit on the properties of phenothiazine-based DSSCs. The photophysical measurements and the theoretical calculations show that the introduction of benzothiadiazole unit to the D−π−A-based dye molecules can broaden the absorption spectrum and strength the hole and electron transfer. However, the device performance is not improved, and the PCE is even reduced. This unexpected result is related to the ICT characteristics of dyes and the electronic lifetime of the devices. The lower q_{CT} and molar extinction coefficient of dye and shorter electron lifetime in the device were the critical reasons for the poor performance of the **PTZ-5** cell. In short, the introduction of benzothiadiazole can improve the spectral response range of the original D−π−A-type dye. However, it is not guaranteed that the photoelectric conversion efficiency will improve. It is necessary to comprehensively investigate the structure of dye and the performance of the device, such as the ICT process of dye and the lifetime of the excited electrons. Our studies thus provide important references for future research on the molecular engineering of phenothiazine-based highly efficient DSSCs.

EXPERIMENTAL SECTION

Characterization. ^{1}H NMR was obtained using a Bruker AM 500 spectrometer. Electronic absorption spectra and emission spectra were recorded on Agilent G1103A and Perkin Elmer LS55 luminescence spectrophotometers, respectively. The cyclic voltammetry (CV) measurements were performed using a computer-controlled CHI660C electrochemical workstation with a three-electrode system. All potentials were reported against the ferrocene/ferrocenium (Fc/Fc^+) reference.[38]

Table 2. Calculated Excitation Energies, λ_{max}, Oscillator Strengths (f), and Main Transition Assignments for PTZ-3 and PTZ-5

dye	state	transition assignments[a]	E (eV)[λ_{max} (nm)]	f
PTZ-3	$S_0 \rightarrow S_1$	60.1% H → L, 24% H − 1 → L	2.78[446]	1.1068
	S0 → S2	38% H → L, 33% H − 1 → L + 1, 12% H − 1 → L + 2	4.27[290]	0.3627
PTZ-5	S0 → S1	51% H → L, 19% H − 1 → L	2.46[504]	0.8936
	S0 → S2	57.5% H → L + 2, 27.5% H − 2 → L	3.62[343]	0.2115

[a]H = HOMO, L = LUMO, H − 1 = HOMO − 1, L + 1 = LUMO + 1, H − 2 = HOMO − 2, and L + 2 = LUMO + 2.

https://dx.doi.org/10.1021/acsomega.0c05887
ACS Omega 2021, 6, 6817−6823

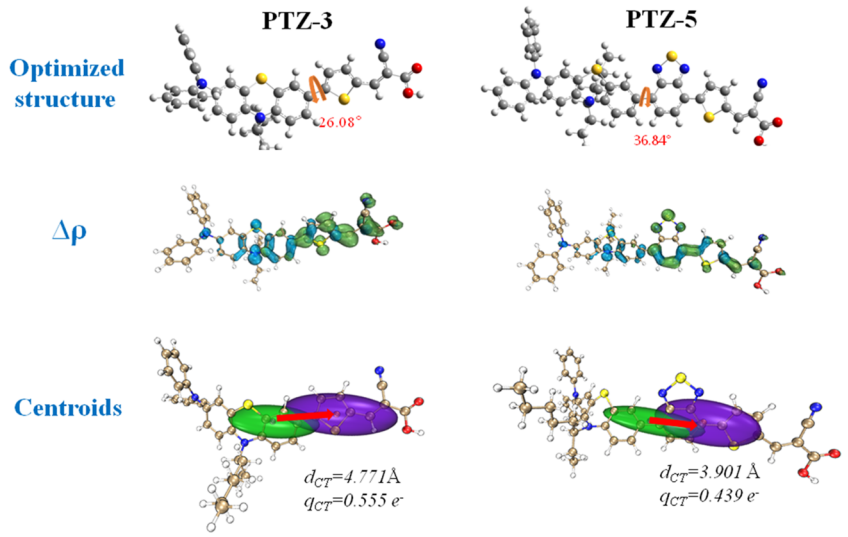

Figure 7. Simulated optimized structure and computed hole (blue)−electron (green) distribution map ($\Delta\rho$) and charge density difference map (centroids) of **PTZ-3** and **PTZ-5**.

Table 3. Computed Charge Transfer Parameters of PTZ-3 and PTZ-5 in the THF Solvent Predicted PBE0/6-311G(d)/SMD Level of Theory

dyes	d_{CT} (Å)[a]	q_{CT} (e^-)[b]	t (Å)[c]	H (Å)[d]
PTZ-3	4.771	0.5551	1.077	3.694
PTZ-5	3.901	0.439	−0.541	4.442

[a]d_{CT} (in Å): length of charge transfer. [b]q_{CT} (in e^-): amount of transfer electrons. [c]t (in Å): extent of charge separation. [d]H (in Å): half sum of the centroid axis length along the D−A direction.

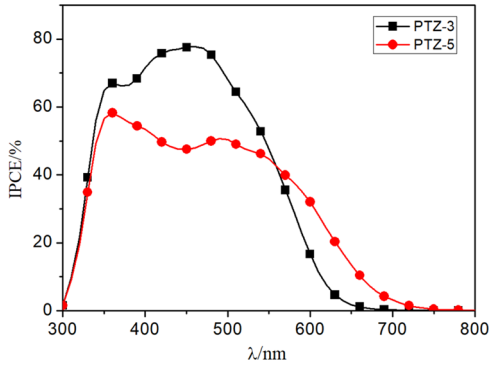

Figure 8. Incident photon-to-electron conversion efficiency (IPCE) spectra of **PTZ-3** cell and **PTZ-5** cell.

Theoretical Calculation. The optimization molecular ground-state geometry and absorption spectra of the **PTZ-3** and **PTZ-5** were obtained in the THF using density functional theory (DFT) and time-dependent density functional theory (TD-DFT) calculation at B3LYP/6-311G(d,p)//B3LYP/6-311G(d) level with Gaussian 09 software, respectively. The detailed methods were described in the previous article.[17,18,40−42]

Device Assembly and Measurements. After treatment, the square TiO_2 electrodes were then immersed into a 300 μM solution of the **PTZ-3** and **PTZ-5** dyes in a mixture of $CHCl_3$ and EtOH (3:7, v/v) for 12 h. The seal uses a 45 mm thick Bynel (DuPont) hot melt gasket to fill the electrolyte into the interior space through a vacuum backfill system. The osmotic electrolyte consisted of 0.6 M dimethylpropylimidazolium iodide, 0.05 M I_2, 0.1 M LiI, and 0.5 M *tert*-butylpyridine in acetonitrile. The detailed processes of device fabrication were very similar to that in the previous articles.[43] Under standard AM 1.5 simulated solar irradiation (WXS155S-10), photocurrent density−voltage (J−V) curves of the solar cell devices were measured by Keithley 2400 Source Meter Instruments. Monochromatic incident photon-to-current conversion efficiency (IPCE) spectra measurement were recorded by a Newport-74125 system (Newport Instruments). Electrochemical impedance spectroscopy (EIS) was measured with a two-electrode system in the dark by Electrochemical Workstation (Zahner IM6e).

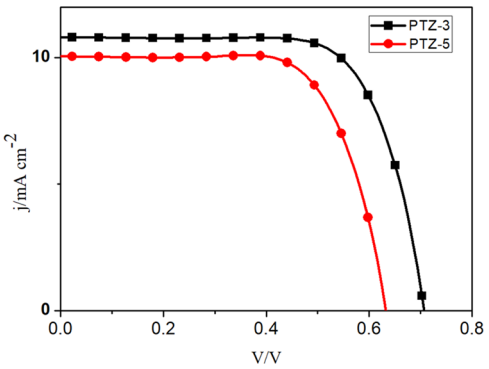

Figure 9. J−V characteristics measured under irradiation of 100 mW·cm^{-2} simulated AM 1.5 sunlight.

Table 4. Photovoltaic Parameters of Cells Measured at an Irradiation of 100 mW·cm^{-2}, Simulated AM 1.5 Sunlight

dyes	V_{oc} (mV)	J_{sc} (mA·cm^{-2})	FF%	PCE%
PTZ-3	710	10.80	69.36	5.35
PTZ-5	640	10.06	69.10	4.43

■ ASSOCIATED CONTENT

Supporting Information

The Supporting Information is available free of charge at https://pubs.acs.org/doi/10.1021/acsomega.0c05887.

https://dx.doi.org/10.1021/acsomega.0c05887
ACS Omega 2021, 6, 6817−6823

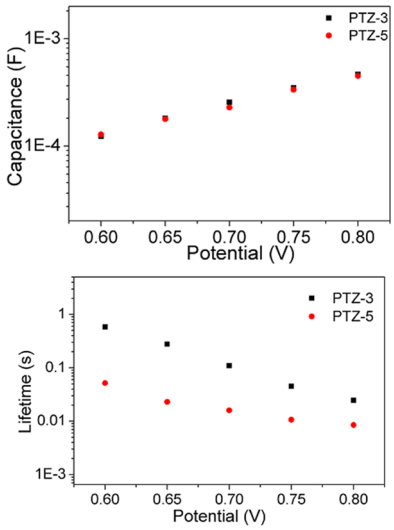

Figure 10. TiO_2 capacitance and electron lifetime as a function of potential based on the **PTZ-3** cell and the **PTZ-5** cell.

Synthetic details and characteristic results for intermediates and target dyes (PDF)

AUTHOR INFORMATION

Corresponding Authors

Yongzhen Wu − *School of Chemistry and Molecular Engineering, East China University of Science and Technology, Shanghai 200237, China*;
Email: wu.yongzhen@ecust.edu.cn

Shuhua Zhang − *College of Chemistry, Guangdong University of Petrochemical Technology, Maoming, Guangdong 525000, China*; orcid.org/0000-0002-1097-1674;
Email: zsh720108@163.com

Haijun Tan − *Guangxi Key Laboratory of Electrochemical and Magneto-chemical Functional Materials, College of Chemistry and Bioengineering, Guilin University of Technology, Guilin 541004, China*; orcid.org/0000-0002-0060-116X;
Email: navytan@glut.edu.cn

Authors

Shengzhong Li − *Guangxi Key Laboratory of Electrochemical and Magneto-chemical Functional Materials, College of Chemistry and Bioengineering, Guilin University of Technology, Guilin 541004, China*

Jingwen He − *Guangxi Key Laboratory of Electrochemical and Magneto-chemical Functional Materials, College of Chemistry and Bioengineering, Guilin University of Technology, Guilin 541004, China*

Huiyun Jiang − *School of Chemistry and Molecular Engineering, East China University of Science and Technology, Shanghai 200237, China*

Shu Mei − *Guangxi Key Laboratory of Electrochemical and Magneto-chemical Functional Materials, College of Chemistry and Bioengineering, Guilin University of Technology, Guilin 541004, China*

Zhenguang Hu − *Guangxi Key Laboratory of Electrochemical and Magneto-chemical Functional Materials, College of Chemistry and Bioengineering, Guilin University of Technology, Guilin 541004, China*

Xiangfei Kong − *Guangxi Key Laboratory of Electrochemical and Magneto-chemical Functional Materials, College of Chemistry and Bioengineering, Guilin University of Technology, Guilin 541004, China*

Miao Yang − *Department of Chemistry, University of Wisconsin-Madison, Madison, Wisconsin 53706, United States*

Complete contact information is available at: https://pubs.acs.org/10.1021/acsomega.0c05887

Notes

The authors declare no competing financial interest.

ACKNOWLEDGMENTS

All authors acknowledge the financial support of this work from the National Natural Science Foundation of China (NSFC 21663010), the Natural Science Foundation of Guangxi (2015GXNSFBA139029), and the special funding for distinguished experts from Guangxi Zhuang Autonomous Region.

REFERENCES

(1) O'Regan, B.; Grätzel, M. A low-cost, High-Efficiency Solar Cell Based on Dye-Sensitized Colloidal TiO_2 Films. *Nature* **1991**, *353*, 737−740.

(2) Hagfeldt, A.; Boschloo, G.; Sun, L.; Kloo, L.; Pettersson, H. Dye-Sensitized Solar Cells. *Chem. Rev.* **2010**, *110*, 6595−6663.

(3) Li, X.; Zhang, X.; Hua, J.; Tian, H. Molecular Engineering of Organic Sensitizers with o,p-dialkoxyphenyl-based Bulky Donors for Highly Efficient Dye-Sensitized Solar Cells. *Mol. Syst. Des. Eng.* **2017**, *2*, 98−122.

(4) Cole, J. M.; Pepe, G.; Al Bahri, O. K.; Cooper, C. B. Cosensitization in Dye-Sensitized Solar Cells. *Chem. Rev.* **2019**, *119*, 7279−7327.

(5) Zeng, K.; Tong, Z.; Ma, L.; Zhu, W.-H.; Wu, W.; Xie, Y. Molecular Engineering Strategies for Fabricating Efficient Porphyrin-Based Dye-Sensitized Solar Cells. *Energy Environ. Sci.* **2020**, *13*, 1617−1657.

(6) Li, L. L.; Diau, E. W. Porphyrin-Sensitized Solar Cells. *Chem. Soc. Rev.* **2013**, *42*, 291−304.

(7) Mathew, S.; Yella, A.; Gao, P.; Humphry-Baker, R.; Curchod, B. F. E.; Ashari-Astani, N.; Tavernelli, I.; Rothlisberger, U.; Nazeeruddin, M. K.; Grätzel, M. Dye-Sensitized Solar Cells with 13% Efficiency Achieved through the Molecular Engineering of Porphyrin Sensitizers. *Nat. Chem.* **2014**, *6*, 242−247.

(8) Zeng, K.; Tang, W.; Li, C.; Yingying, C.; Xie, Y.; et al. Systematic Optimization of the Substituents on the Phenothiazine Donor of Doubly Strapped Porphyrin Sensitizers: An Efficiency over 11% Unassisted by Any Cosensitizer or Coadsorbent. *J. Mater. Chem. A* **2019**, *7*, 20854−20860.

(9) Gao, F. W. Y.; Shi, D.; Zhang, J.; Wang, M.; Jing, X.; Humphry-Baker, R.; Wang, P.; Zakeeruddin, S. M.; Grätzel, M.; et al. Enhance the Optical Absorptivity of Nanocrystalline TiO_2 Film with High Molar Extinction Coefficient Ruthenium Sensitizers for High Performance Dye-Sensitized Solar Cells. *J. Am. Chem. Soc.* **2008**, *130*, 10720−10728.

(10) Chou, C. H. F.; Yeh, H.; Wu, H.; Chi, Y.; Clifford, J. N.; Palomares, E.; Liu, S.; Chou, P.; Lee, G.; et al. Highly Efficient Dye-Sensitized Solar Cells Based on Panchromatic Ruthenium Sensitizers with Quinolinylbipyridine Anchor. *Angew. Chem., Int. Ed.* **2014**, *53*, 178−183.

(11) Hara, K.; Kurashige, M.; Dan-oh, Y.; Kasada, C.; Shinpo, A.; Suga, S.; Sayama, K.; Arakawa, H. Design of New Coumarin Dyes Having Thiophene Moieties for Highly Efficient Organic-Dye-Sensitized Solar Cells. *New J. Chem.* **2003**, *27*, 783−785.

(12) Hara, K.; Sato, T.; Katoh, R.; Furube, A.; Yoshihara, T.; Murai, M.; Kurashige, M.; Ito, S.; Shinpo, A.; Suga, S.; Arakawa, H. Novel

https://dx.doi.org/10.1021/acsomega.0c05887
ACS Omega 2021, 6, 6817−6823

Conjugated Organic Dyes for Efficient Dye-Sensitized Solar Cells. *Adv. Funct. Mater.* **2005**, *15*, 246−252.
(13) Ito, S.; Zakeeruddin, S. M.; Humphry-Baker, R.; Liska, P.; Charvet, R.; Comte, P.; Nazeeruddin, M. K.; Péchy, P.; Takata, M.; Miura, H.; Uchida, S.; Grätzel, M. High-Efficiency Organic-Dye-Sensitized Solar Cells Controlled by Nanocrystalline-TiO_2 Electrode Thickness. *Adv. Mater.* **2006**, *18*, 1202−1205.
(14) Hagberg, D. P.; Yum, J.H.; Lee, H.; De Angelis, F.; Marinado, T.; Karlsson, K. M.; Humphry-Baker, R.; Sun, L.; Hagfeldt, A.; Grätzel, M.; Nazeeruddin, M. K. Molecular Engineering of Organic Sensitizers for Dye-Sensitized Solar Cell Applications. *J. Am. Chem. Soc.* **2008**, *130*, 6259−6266.
(15) Zhu, W.; Wu, Y.; Wang, S.; Li, W.; Li, X.; Chen, J.; Wang, Z.-s.; Tian, H. Organic D−A−π−A Solar Cell Sensitizers with Improved Stability and Spectral Response. *Adv. Funct. Mater.* **2011**, *21*, 756−763.
(16) Sharmoukh, W.; Cong, J.; Gao, J.; Liu, P.; Daniel, Q.; Kloo, L. Molecular Engineering of D-D-pi-A-Based Organic Sensitizers for Enhanced Dye-Sensitized Solar Cell Performance. *ACS Omega* **2018**, *3*, 3819−3829.
(17) Tan, H.; Cai, D.; Liu, Z.; Zhong, F.; Lv, H.; Zhang, X.; Yang, S.; Pan, C. Effects of 2-hexylthiophene on the Performance of Triphenylamine based Organic Dye for Dye-Sensitized Solar Cells. *Synth. Methods* **2016**, *214*, 56−61.
(18) Tan, H.; Pan, C.; Wang, G.; Wu, Y.; Zhang, Y.; Yu, G.; Zhang, M. A Comparative Study on Properties of Two Phenoxazine-Based Dyes for Dye-Sensitized Solar Cells. *Dyes Pigm.* **2014**, *101*, 67−73.
(19) Tan, H.; Pan, C.; Wang, G.; Wu, Y.; Zhang, Y.; Zou, Y.; Yu, G.; Zhang, M. Phenoxazine-Based Organic Dyes with Different Chromophores for Dye-Sensitized Solar Cells. *Org. Electron.* **2013**, *14*, 2795−2801.
(20) Wang, G.; Hu, Y.; Chen, Y.; Liao, X.; Li, Z.; Chen, X.; Wang, X.; Liu, B. Effect of Multidonor and Insertion Position of a Chromophore on the Photovoltaic Properties of Phenoxazine Dyes. *ACS Omega* **2020**, *5*, 22621−22630.
(21) Kakiage, K.; Aoyama, Y.; Yano, T.; Oya, K.; Fujisawa, J.; Hanaya, M. Highly-Efficient Dye-Sensitized Solar Cells with Collaborative Sensitization by Silyl-Anchor and Carboxy-Anchor Dyes. *Chem. Commun.* **2015**, *51*, 15894−15897.
(22) Zhang, L.; Yang, X.; Wang, W.; Gurzadyan, G. G.; Li, J.; Li, X.; An, J.; Yu, Z.; Wang, H.; Cai, B.; Hagfeldt, A.; Sun, L. 13.6% Efficient Organic Dye-Sensitized Solar Cells by Minimizing Energy Losses of the Excited State. *ACS Energy Lett.* **2019**, *4*, 943−951.
(23) Ji, J. M.; Zhou, H.; Eom, Y. K.; Kim, C. H.; Kim, H. K. 14.2% Efficiency Dye-Sensitized Solar Cells by Co-sensitizing Novel Thieno[3,2-b]indole-Based Organic Dyes with a Promising Porphyrin Sensitizer. *Adv. Energy Mater.* **2020**, *10*, No. 2000124.
(24) Joly, D.; Pellejà, L.; Narbey, S.; Oswald, F.; Demadrille, R. A Robust Organic Dye for Dye Sensitized Solar Cells Based on Iodine/Iodide Electrolytes Combining High Efficiency and Outstanding Stability. *Sci. Rep.* **2014**, *4*, No. 4033.
(25) Lu, X.; Lan, T.; Qin, Z.; Wang, Z. S.; Zhou, G. A Near-Infrared Dithieno[2,3-a:3′,2′-c]Phenazine-Based Organic Co-Sensitizer for Highly Efficient and Stable Quasi-Solid-State Dye-Sensitized Solar Cells. *ACS Appl. Mater. Interfaces* **2014**, *6*, 19308−19317.
(26) Baheti, A.; Thomas, K. R. J.; Li, C. T.; Lee, C. P.; Ho, K. C. Fluorene-Based Sensitizers with a Phenothiazine Donor: Effect of Mode of Donor Tethering on the Performance of Dye-Sensitized Solar Cells. *ACS Appl. Mater. Interfaces* **2015**, *7*, 2249−2262.
(27) Alibabaei, L.; Kim, J. H.; Wang, M.; Pootrakulchote, N.; Teuscher, J.; Di Censo, D.; Humphry-Baker, R.; Moser, J. E.; Yu, Y. J.; Kay, K. Y.; Zakeeruddin, S. M.; Grätzel, M. Molecular Design of Metal-Free D−π−A Substituted Sensitizers for Dye-Sensitized Solar Cells. *Energy Environ. Sci.* **2010**, *3*, 1757−1764.
(28) Kim, B. G.; Zhen, C. G.; Jeongjeong, E.; Kieffer, J.; Kim, J. Organic Dye Design Tools for Efficient Photocurrent Generation in Dye-Sensitized Solar Cells: Exciton Binding Energy and Electron Acceptors. *Adv. Funct. Mater.* **2012**, *22*, 1606−1612.
(29) Wu, Y.; Zhang, X.; Li, W.; Wang, Z.-S.; Tian, H.; Zhu, W. Hexylthiophene-Featured D−A−π−A Structural Indoline Chromophores for Coadsorbent-Free and Panchromatic Dye-Sensitized Solar Cells. *Adv. Energy Mater.* **2012**, *2*, 149−156.
(30) Funabiki, K.; Mase, H.; Hibino, A.; Tanaka, N.; Mizuhata, N.; Sakuragi, Y.; et al. Synthesis of A Novel Heptamethine-Cyanine Dye for Use in Near-Infrared Active Dye-Sensitized Solar Cells with Porous Zinc Oxide Prepared at Low Temperature. *Energy Environ. Sci.* **2011**, *4*, 2186−2192.
(31) Do, K.; Kim, D.; Cho, N.; Paek, S.; Song, K.; Ko, J. New Type of Organic Sensitizers with a Planar Amine Unit for Efficient Dye-Sensitized Solar Cells. *Org. Lett.* **2012**, *14*, 222−225.
(32) Cheng, H. M.; Hsieh, W. F. High-Efficiency Metal-Free Organic-Dye-Sensitized Solar Cells with Hierarchical Zno Photoelectrode. *Energy Environ. Sci.* **2010**, *3*, 442−447.
(33) Wu, Y.; Marszalek, M.; Zakeeruddin, S.; Zhang, Q.; Tian, H.; et al. High-Conversion-Efficiency organic Dye-Sensitized Solar Cells: Molecular Engineering on D−A−P−A Featured Organic Indoline Dyes. *Energy Environ. Sci.* **2012**, *5*, 8261−8272.
(34) Li, W.; Wu, Y.; Zhang, Q.; Tian, H.; Zhu, W. D−A−π−A Featured Sensitizers Bearing Phthalimide and Benzotriazole as Auxiliary Acceptor: Effect on Absorption and Charge Recombination Dynamics in Dye-Sensitized Solar Cells. *ACS Appl. Mater. Interfaces* **2012**, *4*, 1822−1830.
(35) Chang, D. W.; Lee, H. J.; Kim, J. H.; Park, S. Y.; Park, S. M.; Dai, L.; Baek, J. B. Novel Quinoxaline-Based Organic Sensitizers for Dye-Sensitized Solar Cells. *Org. Lett.* **2011**, *13*, 3880−3883.
(36) Zhu, H.; Li, W.; Wu, Y.; Liu, B.; Zhu, S.; Li, X.; Ågren, H.; Zhu, W. Insight into Benzothiadiazole Acceptor in D−A−π−A Configuration on Photovoltaic Performances of Dye-Sensitized Solar Cells. *ACS Sustainable Chem. Eng.* **2014**, *2*, 1026−1034.
(37) Zhu, H.; Wu, Y.; Liu, J.; Zhang, W.; Wu, W.; Zhu, W. H. D−A−π−A Featured Sensitizers Containing An Auxiliary Acceptor of Benzoxadiazole: Molecular Engineering and Co-Sensitization. *J. Mater. Chem. A* **2015**, *3*, 10603−10609.
(38) He, J.; Pei, H.; Li, H.; Zhang, S.; Zhang, S.; Tan, H.; Hu, Z. Comparative Analysis of Phenothiazine and Phenoxazine Sensitizers for Dye-Sensitized Solar Cells. *Synth. Met.* **2019**, *247*, 228−232.
(39) Roy, J. K.; Kar, S.; Leszczynski, J. Revealing the Photophysical Mechanism of N,N′-Diphenyl-aniline Based Sensitizers with the D−D−π−A Framework: Theoretical Insights. *ACS Sustainable Chem. Eng.* **2020**, *8*, 13328−13341.
(40) Tirado-Rives, J.; Jorgensen, W. L. Performance of B3LYP Density Functional Methods for a Large Set of Organic Molecules. *J. Chem. Theory Comput.* **2008**, *4*, 297−306.
(41) Xu, Z.; Li, Y.; Zhang, W.; Yuan, S.; Hao, L.; Xu, T.; Lu, X. DFT/TD-DFT Study of Novel T Shaped Phenothiazine-Based Organic Dyes for Dye-Sensitized Solar Cells Applications. *Spectrochim. Acta, Part A* **2019**, *212*, 272−280.
(42) Song, Y.; Lu, X.; Sheng, Y.; Zhao, G.; Wang, G.; Geng, Z. Theoretical Investigations On Newly Designed Triphenylamine-Based Donors Applied into the D−π−A And D−A−π−A Type Sensitizers. *J. Comput. Electron.* **2018**, *17*, 1816−1834.
(43) Jiang, H.; Wu, Y.; Islam, A.; Wu, M.; Zhang, W.; Shen, C.; Zhang, H.; Li, E.; Tian, H.; Zhu, W. H. Molecular Engineering of Quinoxaline-Based D−A−pi−A Organic Sensitizers: Taking the Merits of a Large and Rigid Auxiliary Acceptor. *ACS Appl. Mater. Interfaces* **2018**, *10*, 13635−13644.

https://dx.doi.org/10.1021/acsomega.0c05887
ACS Omega 2021, 6, 6817−6823